Cellular Uptake and Nuclear Delivery of Recombinant Adenovirus Penton Base

Saw See Hong,*,†,[1] Bernard Gay,†,[1] Lucie Karayan,†,[1] Marie-Christine Dabauvalle,‡ and Pierre Boulanger*,†,[2]

*Laboratoire de Virologie et Pathogénèse Virale, CNRS UMR 5537, Faculté de Médecine RTH Laennec, Rue Guillaume Paradin, 69008 Lyon, France; †Laboratoire de Virologie Moléculaire, Faculté de Médecine, Institut de Biologie, 34060 Montpellier, France; and ‡Department of Cell and Developmental Biology, Theodor-Boveri-Institute, University of Würzburg Am Hubland, D-97074 Würzburg, Germany

An Ad2 capsid component, the penton base, expressed as recombinant protein, was found to be capable of affecting the entire entry pathway of adenovirion in HeLa cells, i.e., cell attachment, endocytosis, vesicular escape, intracytoplasmic movement, and translocation through the nuclear pore complex. Data with pentamerization-defective mutants suggested that none of these successive steps depended upon penton base pentamer status, indicating that the peptide domains responsible for these functions were carried by the monomer. Observations performed with wild-type (WT) and an integrin-binding-site double-mutant (K288E340) suggested that the penton base could enter the cell via an alternative, RGD- and LDV-independent, pathway. Of three mutants that were found to be defective in nuclear addressing in insect cells, only one, W165H, was also altered in nuclear transport in HeLa cells. The other two, W119H and RRR547EQQ, showed a WT pattern of nuclear localization in HeLa cells, suggesting that the region including tryptophan-119 and the basic signal at position 547 did not act as a nuclear localization signal in the human cell context. The integrity of cellular structures and the cytoskeleton seemed to be required for the vectorial movement and nuclear import of WT penton base, as suggested by experiments using permeabilized HeLa cells, isolated nuclear membranes, and cytoskeleton-targeted drugs. © 1999 Academic Press

Key Words: adenovirus serotype 2 (Ad2); penton base; endocytosis; vesicular escape; nuclear import; nuclear pore complex; membrane translocation; protein trafficking.

INTRODUCTION

Adenoviruses (Ad) are nonenveloped, double-stranded DNA viruses that replicate and assemble their virions within the nucleus of infected cells. The virion is composed of 252 capsomeres—240 hexons and 12 pentons; the latter are located at the 12 vertices of the icosahedral capsid (reviewed in Nermut, 1984, Stewart *et al.,* 1991). The penton is a heteromeric protein formed of the penton base, a homopentameric protein, noncovalently linked to a homotrimeric protein, the fiber (Boudin and Boulanger, 1982; Ruigrok *et al.,* 1990; Stouten *et al.,* 1992). The early phase of the Ad lytic cycle has been divided into the following steps: (i) attachment of the infectious virus particle to primary cell receptors via its fiber projections; (ii) binding of the penton base capsomere to plasma membrane integrins, acting as secondary receptors; (iii) endocytosis into clathrin-coated vesicles; (iv) conformational change and partial disruption of the capsid within the endocytic vesicle; (v) endosomolysis and escape from the endosome; (vi) transit across the cytoplasm to reach the nucleus; and (vii) entry into the nucleoplasm through the nuclear pore (Greber *et al.,* 1993; Greber and Kasamatsu, 1996; Seth *et al.,* 1986; Varga *et al.,* 1991; Whittaker and Helenius, 1998).

Although it is reasonable to assume that the complex process of entry and intracellular transit involves several virion structural proteins carrying specific signals, it appears that the penton capsomere (penton base and fiber) carries most of the functions required for the early steps of the cellular entry pathway. Thus, Ad–cell binding in step (i) is mediated by the terminal sphere of the fiber (the fiber knob) protruding from the penton base capsomere and fiber receptors present at the cell surface (Bergelson *et al.,* 1997; Hong *et al.,* 1997; Tomko *et al.,* 1997). The knob serotype is therefore a major determinant of the cell tropism (Defer *et al.,* 1990; Krasnykh *et al.,* 1996; Santis *et al.,* 1999; Stevenson *et al.,* 1995; Xia *et al.,* 1995), even though it is probably not the only viral factor (Roelvink *et al.,* 1998). At the second step (ii), the interaction of RGD and LDV triplet motifs in the penton base with the cell plasma membrane integrins is required to induce or trigger endocytosis. Some cell specificity has been attributed to this process, as the RGD motifs interact with $\alpha v\beta3$, $\alpha v\beta5$, and $\alpha M\beta2$ integrins, and LDV motifs interact with $\alpha4\beta1$ and $\alpha4\beta7$ integrins (Belin and Boulanger, 1993; Hong and Boulanger, 1995; Mathias *et al.,* 1994; Hynes, 1992; Wickham *et al.,* 1993, 1995). The

---

[1] These authors contributed equally to this work.

[2] To whom correspondence and reprint requests should be addressed. Fax: 33 (0)4 78 77 87 51. E-mail: pboulang@infobiogen.fr.

163

mechanisms of endosomal escape (v), transcytoplasmic movement (vi), and traverse of the nuclear pore channel (vii) still remain elusive. However, involvement of the penton base in endosomal escape has been assessed (Seth, 1994a; Seth et al., 1984; Yoshimura, 1985; Yoshimura et al., 1993), as has the participation of cytoskeletal elements in step vi (Belin and Boulanger, 1985, 1987; Dales and Chardonnet, 1973; Defer et al., 1990; Weatherbee et al., 1977; Zhai et al., 1988; Zhang and Schneider, 1994). Furthermore, a functional nuclear localization signal has been identified in hexon, the major Ad capsid protein (Saphire et al., 1995), which could account for the binding of partially uncoated adenoviral DNA, still associated with hexons and core proteins (Greber et al., 1993), to the nuclear pore complex (NPC). Additional peptide sequences containing instructions for other discrete steps of the intracellular migration and compartmentalization of the virions are yet to be determined.

We have expressed the Ad2 penton base protein in baculovirus-infected insect cells and found that the recombinant wild-type (WT) penton base protein (571 residues; PbFL571; Karayan et al., 1994, 1997) apparently retained all the biological properties of the penton base synthesized in Ad2-infected human KB or HeLa cells. It was indistinguishable from HeLa cell-extracted penton base under the electron microscope (EM), and it assembled with coexpressed fiber in vivo in Sf9 cells, to form penton capsomere (Karayan et al., 1994, 1997). Similar to the penton base isolated from Ad-infected HeLa cells, it also interacted with recombinant fiber in vitro and showed the same cell-detaching effect (Bai et al., 1993; Boudin et al., 1979; Karayan et al., 1994, 1997), a consequence of the competition of its RGD triplets with cell adhesion molecules for the conserved SMKDDLW sequence of the integrin β-chains (D'Souza et al., 1994; Hong and Boulanger, 1995).

In the present study, we investigated the interaction of penton base with HeLa cells in culture and its occurrence in the different cellular compartments. Our study was performed using the WT penton base from Ad serotype 2 (Ad2), which has 98% sequence identity with serotype 5 penton base (Neuman et al., 1988), expressed as recombinant proteins isolated from baculovirus-infected insect cells, and several of its mutants (Karayan et al., 1997). We found that the WT penton base protein carried enough information to enter the cell after endocytosis and achieve its self-delivery to the nucleus of HeLa cells in culture, by translocation through the nuclear pore complex, similar to infectious adenovirions. Experiments using permeabilized HeLa cells, cytoskeleton-targeted drugs, and isolated nuclear membranes in vitro suggested that the integrity of the cell structure and of the cytoskeleton microfilaments and microtubules was required for the vectorial movement of the penton base across the cell and for its nuclear delivery.

RESULTS

Cellular uptake of Ad2 penton base by HeLa cells

Penton base capsomeres in Ad capsids interact with cell plasma membrane integrins, considered as secondary receptors for the virus, but isolated penton base, used as soluble recombinant protein, has also been found to possess HeLa cell binding capacity at 0°C (Karayan et al., 1997). However, the fate of cell surface-adsorbed penton base molecules at 37°C had not been investigated. Recombinant WT penton base protein was thus incubated with HeLa cell monolayers for 30 min at 37°C, at a total penton base protein input of 12×10^{12} ligand molecules per 10^6 cell sample, corresponding to about a 100-fold excess over the theoretical number of cell receptors reported for penton base protein (9×10^4 per cell; Wickham et al., 1993). Cell-associated penton base, as assayed by sodium dodecyl sulfate–polyacrylamide gel electrophoresis (SDS–PAGE) and immunoblot analysis of whole-cell lysates, was found to range from 1 to 1.5% of the penton base protein input, i.e., 1.2×10^5 to 1.8×10^5 molecules of penton base protein per cell. Most of the cell-associated penton base resisted several cycles of rinsing with PBS with or without mild detergent (0.2% NP-40) or trypsin (10 μg/ml), suggesting that the fraction of protease-resistant penton base sedimenting with the cell pellet had been adsorbed into the cells.

To assess the cellular uptake of the penton base protein and its intracellular distribution, HeLa cell monolayers were incubated with penton base for 15 min at 37°C, rinsed with prewarmed culture medium, and further incubated at 37°C for different periods of time, ranging from 10 to 120 min. The cells were then lysed, fractionated into a nuclear pellet (N), an intermediate fraction containing large organelles, membranes, and endosomal vesicles (V), and the cytosolic supernatant (C), and the three subcellular fractions were immunologically assayed for penton base protein, as above. At 10–20 min (Fig. 1a, lanes 6–8), a significant proportion of the penton base was already pelletable with the nuclei (N), but the majority was found in the endosomal and vesicular fraction (V). At 60 min, the proportion of penton base recovered from the nuclear pellet increased (Fig. 1a, lanes 9–11), and at 2 h, most of the penton base was found in the nuclear and cytoplasmic (C) fractions (Fig. 1a, lanes 12–14). The progressive change in cellular distribution of penton base protein and its increase in the nuclear compartment during the incubation period suggested the occurrence of a cell entry process and vectorial movement toward the nucleus.

The possible intracellular persistence of penton base or, the contrary, its clearance from HeLa cells was also investigated, using a prolonged chase period at 37°C. HeLa cell monolayers were taken at half-confluence and incubated with the penton base for 15 min at 37°C as above, and then, after removal of nonadsorbed penton
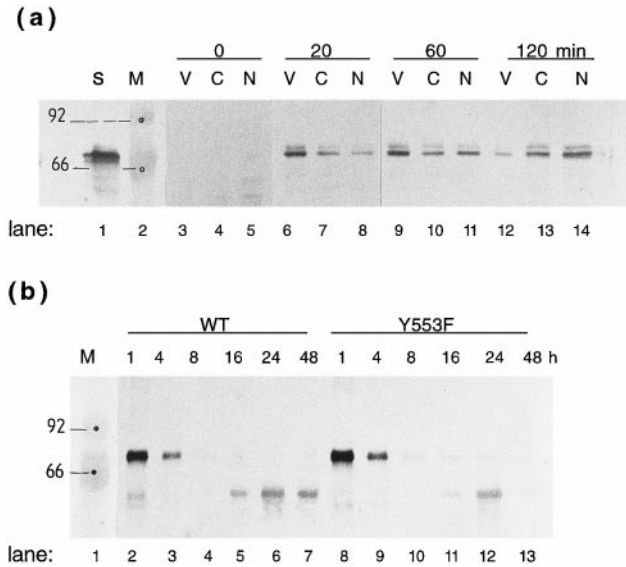
FIG. 1. (a) Distribution of recombinant penton base protein in cellular compartments of HeLa cells. Penton base protein, adsorbed to HeLa cells for 15 min at 37°C, was immunologically assayed in the vesicular and membrane fraction (V), the cytosolic supernatant (C), and the nuclear pellet (N) at different times of chase at 37°C (lanes 6–14: 20, 60, and 120 min, respectively). Lane 1, aliquot of cell culture medium containing unadsorbed penton base (S). Lane 2, prestained molecular mass markers (M), showing 92- and 66-kDa marker proteins. Lanes 3–5, zero time point samples from control HeLa cells harvested prior to incubation with penton base. (b) Fate of intracellular penton base in HeLa cells. Half-confluent HeLa cell monolayers were incubated at 37°C for 15 min with recombinant penton base, WT (lanes 2–7), or Y553F mutant (lanes 8–13). Cells were rinsed and further incubated in culture medium for 48 h at 37°C (chase), and samples were withdrawn at different time intervals. Whole-cell lysates were analyzed by SDS–PAGE and immunoblotting with penton base antibody. The figures at the top indicate the times of the chase period (in h), and the figures on the left represent the molecular mass markers of 92 and 66 kDa (lane 1, M).

base, cells were further maintained in culture until 72 h, with renewal of the medium at 24 and 48 h. Penton base protein of apparent M_r 80-kDa was still detected in cell lysates after 4 h, but barely detectable at 8 h (Fig. 1b, lanes 2–4). However, between 8 and 48 h, most of the intracellular penton base protein was converted to a discrete 60-kDa species, which likely represented a major cleavage product (Fig. 1b, lanes 5–7). The 60-kDa band decreased at 48 h and was no longer detected at 72 h (not shown), suggesting that the penton base was cleared from the cells mainly in the form of a 60-kDa cleavage product. A pentamerization-defective mutant, Y553F, occurring as penton base monomers, was used for comparison. The Y553F pattern was similar, although the 60-kDa species seemed to disappear at a faster rate (Fig. 1b, lanes 8–13). This suggested that penton base monomers could enter the cell as efficiently as pentamers (compare lanes 2 and 8, showing WT and Y553F, respectively), but that the penton base monomers were less resistant to proteolysis.

The possible cytotoxicity of penton base during the chase period following its cellular uptake was explored by flow cytometry. No apparent detrimental effect of penton base on HeLa cell growth and viability was detectable, as the percentage of dead cells in penton base-treated cells at 2, 8, 16, 24, and 48 h of postincubation was not significantly different from that in mock-treated cells (data not shown).

## Internalization and cellular compartmentalization of penton base

The definition of the subcellular fractions analyzed above was essentially operational and had the main advantage of providing a kinetic representation of the fate of intracellular penton base after its cellular uptake. However, compartment leakage usually occurred during cell fractionation, and cross-contaminations were inevitable for subcellular fractions obtained by differential centrifugation. A refined analysis of the cell entry and compartmentalization of penton base was then performed by immunoelectron microscopy (IEM) using indirect immunogold labeling or direct gold labeling of the penton base protein. As shown in Fig. 2, penton base protein was detected by IEM in virtually all compartments of HeLa cells after a 30-min incubation period at 37°C. Gold grains of penton base-bound antibody were found at the plasma membrane (Figs. 2a and 2c), as well as within intracytoplasmic vacuoles (Figs. 2b, 2d, 2e, and 2f), and in significant amounts within the cytoplasm and nucleoplasm (Figs. 2b and 2g). Endosomal release was suggested by discontinuities of the vesicular membrane, with the occurrence of immunogold-labeled material on both the inner and the outer leaflets of the disrupted membrane (Figs. 2b, 2d, and 2f). Most of the large intracellular vacuoles in which penton base labeling was detected were apparently devoid of a clathrin layer, but typical clathrin-coated, small vesicles that contained gold grains were also observed (Fig. 2c), as described for adenovirions (Chardonnet and Dales, 1970). Cellular internalization and vesicular and nuclear localization of penton base in HeLa cells were also evidenced by immunofluorescence (IF) microscopy using a confocal laser system (as shown in Fig. 6a).

Examination of the plasma membrane under the EM after immunogold labeling of cell sections revealed gold grains on both sides of the membrane double leaflet (as illustrated in Figs. 2a and 2c). This could suggest a direct mechanism of entry of penton base across the plasma membrane, as previously postulated to occur for the adenovirion itself (Morgan et al., 1969). However, the detection of penton base antigen by indirect IEM indicates its binding to a primary penton base rabbit antibody molecule, bound itself to a secondary anti-rabbit IgG molecule carrying the 5-nm gold grain tag. The theoretical length of this two-story-high antibody com-
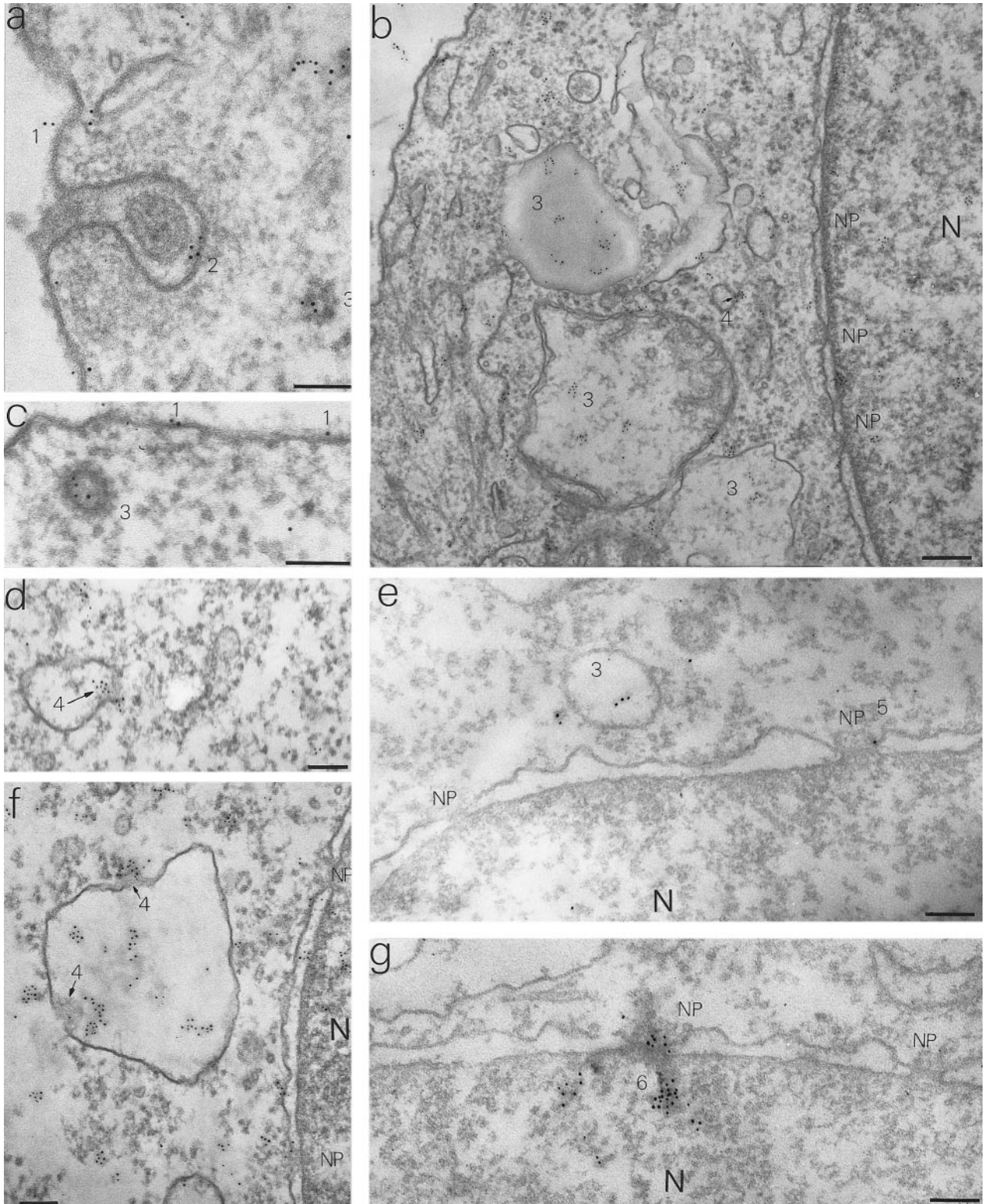
FIG. 2. Immunogold labeling and EM analysis of penton base interaction with HeLa cells and intracellular localization. Recombinant penton base was incubated at 37°C for 30 min with HeLa cell monolayers, and cells were processed for EM. Cell sections were reacted with penton base rabbit antibody and 5-nm gold-conjugated anti-rabbit IgG antibody. The different panels show cellular compartments taken from different areas of cell sections. Hypothetical steps of the penton base entry pathway are arbitrarily numbered as follows: (1) attachment to the cell plasma membrane; (2) endocytosis; (3) intravesicular step; (4) vesicular escape and entry into the cytoplasm; (5) docking at the nuclear pore; (6) translocation across the nuclear pore. Note that clathrin-coated vesicles in (a) and (c) contained gold grain-labeled penton base. Arrows in (b), (d), and (e) point to regions of discontinuities in the endosomal membrane. N, nucleus; C, cytoplasm; NP, nuclear pore. Bar represents 200 nm in (b), and 100 nm in all other panels.
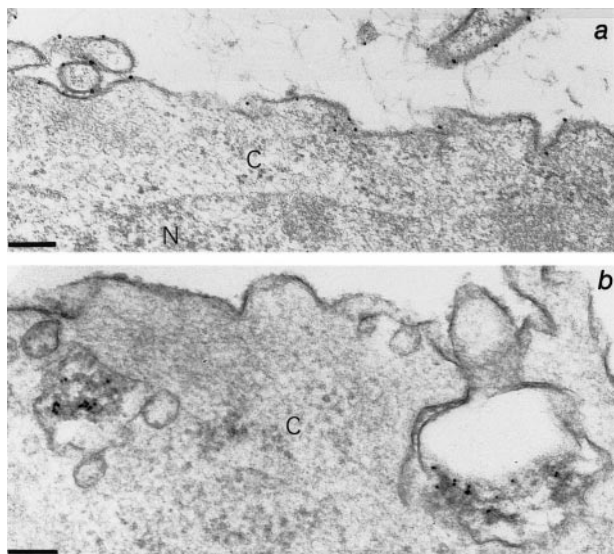
FIG. 3. Direct EM analysis of penton base–HeLa cell interaction. Penton base protein tagged with 10-nm gold was incubated with HeLa cell monolayers at 0°C for 2 h (a) and shifted to 37°C for 30 min (b). N, nucleus; C, cytoplasm. Bar represents 100 nm.

plex separating the penton base antigen from the gold grain (about 40 nm; Davies and Padlan, 1990) largely exceeded the thickness of the plasma membrane double leaflet (5–6 nm). Thus, one could not exclude a possible tilting of gold-labeled immunoglobulin molecules over the plasma membrane, which could simulate an intracellular localization of the penton base molecule.

To eliminate this type of ambiguity, we then used penton base molecules labeled with colloidal gold tag prior to their incubation with HeLa cells, to directly visualize penton base protein under the EM without an intermediate antibody. This experiment also tested the capacity of penton base to serve as a carrier for a molecule of similar size: the mean diameter of the colloidal gold tag (10 nm) was of the same order of magnitude as the size of the penton base, reported to be 9 nm in diameter by negative staining analysis under the EM (Ruigrok et al., 1990) or 11.2×12.4 nm from image reconstruction data (Stewart et al., 1993, 1997). After a 2-h incubation period with HeLa cells at 0°C, numerous gold-tagged penton base molecules were seen at the cell surface (Fig. 3a). At 37°C, gold-tagged penton base molecules were endocytosed by HeLa cells, as shown by the occurrence of a number of gold grains within vacuoles (Fig. 3b). However, very few gold grains were detected in the cytoplasm and in the nucleoplasm after 30 min at 37°C. This suggested that gold-tagged penton base molecules were less efficiently internalized and addressed to the nucleus than nontagged penton base, an observation that might have significant implications if Ad penton base protein is envisaged to be used as a vehicle for gene therapy.

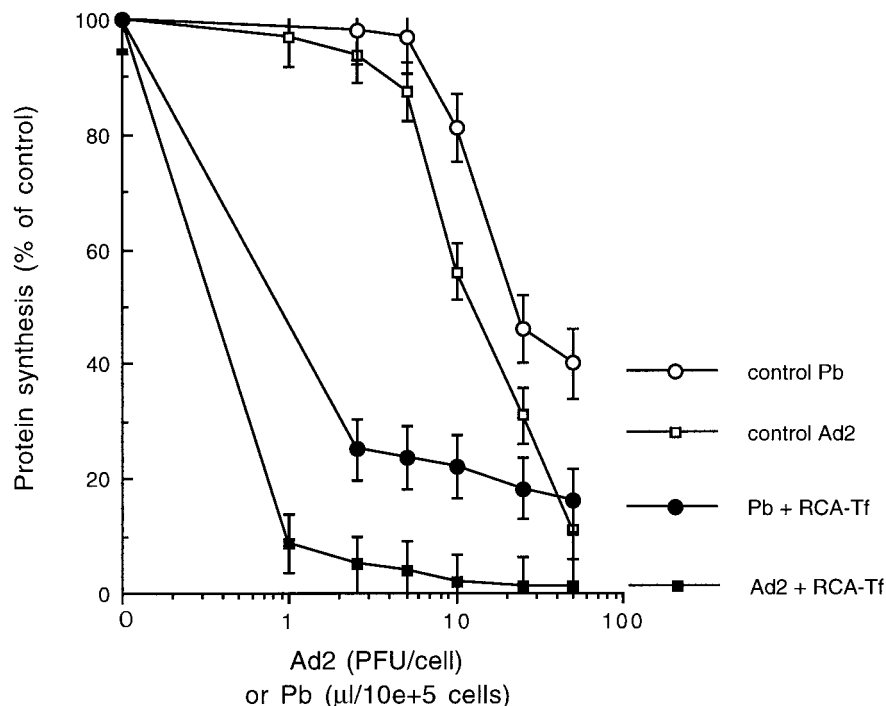## Vesicular release of coendocytosed penton base and toxin molecules

The possible release of penton base from the endosome into the cytoplasm by translocation and/or vesicular membrane disruption, as suggested by EM analysis (Figs. 2b, 2d, and 2f), was further investigated using a bioassay based on the endosomal release of coendocytosed toxins with inhibitory effects on host cell protein synthesis (FitzGerald et al., 1983a,b; Seth et al., 1984, 1985; Seth, 1994b). We used ricin agglutinin (RCA), a heterodimeric glycoprotein with a cytotoxic A chain linked by a disulfide bond to a B chain, a lectin that binds to a galactose-containing receptor (Olsnes and Phil, 1982). Internalization of ricin by sensitive cells leads to reduction of the disulfide bond, separation of the chains, and translocation of the toxic A chain to the cytoplasm, where it inhibits protein synthesis via N-glycosidase activity on 28S rRNA (Endo and Tsurugi, 1987). We coupled RCA to human transferrin (Tf) via a streptavidin bridge, such that it would follow the well-defined pathway of Tf receptor endocytosis (Curiel et al., 1991; FitzGerald et al., 1983a).

We found that RCA–Tf alone decreased HeLa cell protein synthesis by only 30–35% under our experimental conditions. However, in the presence of Ad2 virions, its cytoxicity increased significantly, with 90% inhibition at 2 PFU/cell (Fig. 4). WT penton base protein also increased the cytoxicity of RCA–Tf conjugate; at 0.5–1.0 μg per 10^5 cells, a concentration at which the intrinsic cytopathic effect of penton base was negligible, protein synthesis was reduced to 20% of control (Fig. 4). The penton base activity was abolished after being heated to 56°C for 30 min, suggesting that it required native protein conformation. These results suggested that isolated penton base protein facilitated the internalization of macromolecules, as does the adenovirion itself (Defer et al., 1990; Karayan et al., 1997), but with a much lower efficiency. Considering that about 1% of the penton base input entered the cells, and that one infecting unit of Ad2 (1 PFU) corresponded to about 30–50 physical particles containing 12 penton capsomeres each, the level of endosomal release of RCA–Tf was 1000 to 2000 times more efficient with virions than with free penton base protein. This would suggest that other capsid components could participate in the vesicular release process or, alternatively, that the conformation and biological properties could be different for free and virion-incorporated penton base or both.

Interaction of the penton base with the nuclear pore complex in situ

Detection of the penton base in the HeLa cell nucleus by cell fractionation (Fig. 1) and IEM (Fig. 2) as early as 30 min after its input suggested an efficient nuclear addressing and passage of penton base molecules across the nuclear pores. Nuclear membranes of HeLa

FIG. 4. Cytotoxic assay of vesicular release of Ad2 virions and isolated penton base capsomeres. In control experiments, the intrinsic cytotoxicity of Ad2 virion and penton base protein was determined by incubation of HeLa cell monolayers with increasing m.o.i. of Ad2 (control Ad2) or increasing input of penton base protein (control Pb) in the absence of toxin. In two other sets of samples, cytotoxicity of transferrin-conjugated ricin (RCA), at constant amounts of 1 μg per 10^5 cells, was assessed in the presence of increasing inputs of Ad2 (Ad2 + RCA–Tf) or penton base (Pb + RCA–Tf). The level of cellular protein synthesis was determined by radiolabeling with [^{35}S]methionine+cysteine. Results were normalized and are expressed as percentage of protein-incorporated radioactivity in control samples without RCA (open symbols) or with RCA (solid symbols). On the x-axis, 10 μl of penton base solution corresponds to 1 μg penton base protein.
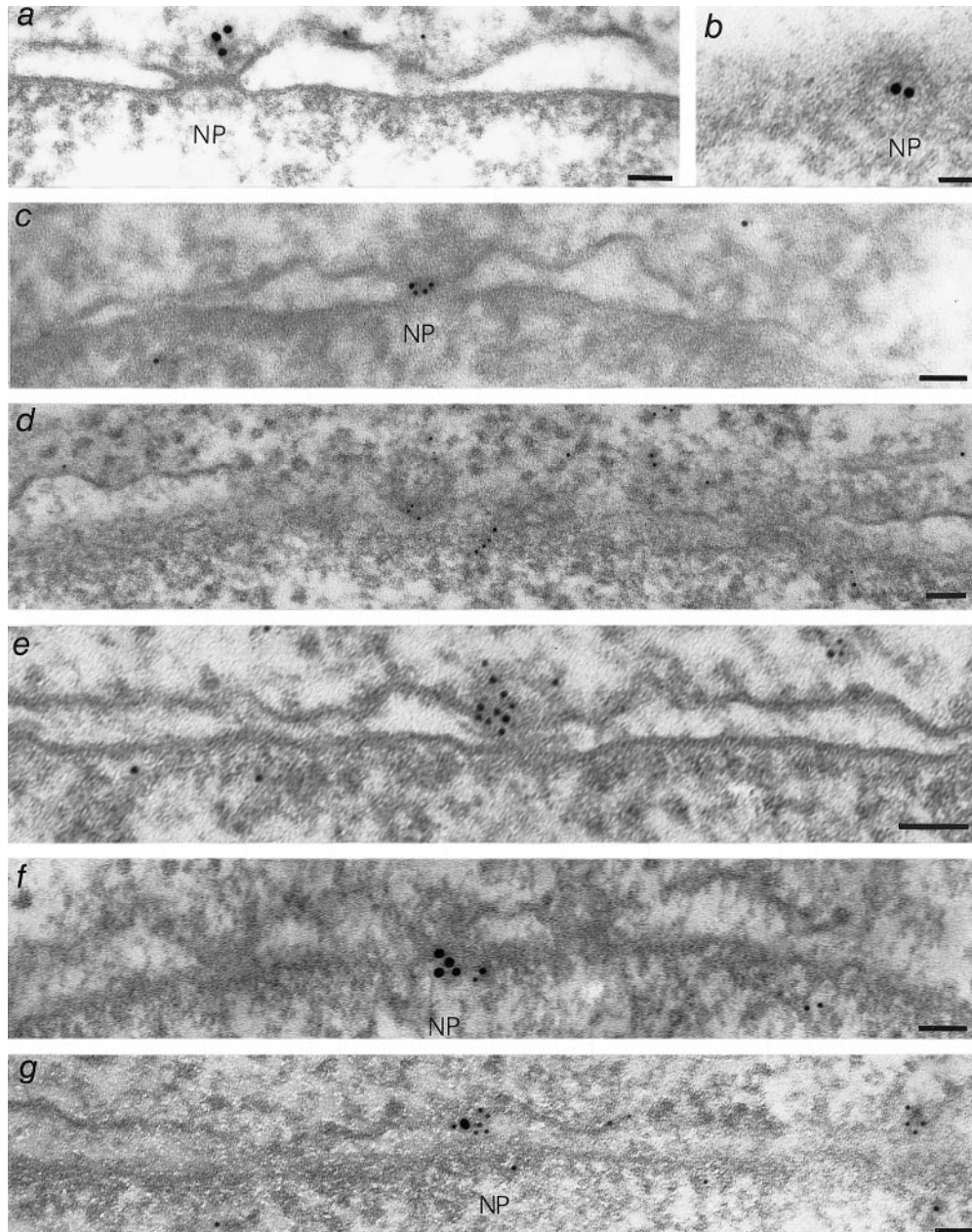
cells incubated with the penton base were thus further analyzed by IEM with special focus on NPC, using single or double immunogold labeling. In the many electron micrographs observed, gold grains were seen in close association with NPC, and on several occasions, multiple gold grains were found on both the cytoplasmic and the nucleoplasmic sides of nuclear pores, as well as within the central channel viewed in cross (Figs. 2e–2g, and 5c) or tangential sections (Figs. 5d and 5e). This was confirmed by double immunogold labeling experiments, in which penton base rabbit antibody was detected by 5-nm gold-labeled conjugate, whereas PI1, a mouse monoclonal antibody directed against the nuclear pore glycoprotein p62, was detected by 10-nm gold-labeled conjugate (Figs. 5a and 5b). Several NPC carried double labeling with both 5- and 10-nm gold grains (Figs. 5f and 5g). All these observations strongly suggested a translocation of the penton base molecules through the NPC.

Quantitative analysis of cellular uptake and compartmentalization of WT and mutant penton base

Quantification of penton base protein in the three major cell compartments, intracytoplasmic vacuoles (V), cytosol (C), and nucleus (N), was performed using IEM, by counting the penton base-associated immunogold

grains on a series of cell sections (Carrière et al., 1995; Huvent et al., 1998; Karayan et al., 1997). The results, expressed in terms of grain density (i.e., the number of grains per square micrometer of cell section area), are shown in Table 1. After 30 min of incubation with HeLa cells at 37°C, WT penton base was found in abundance within the vesicular compartment (more than 50%), including large endosomes as well as smaller vacuoles. The other half was distributed almost equally between cytoplasm and nucleus. This corresponded to the pattern of cellular distribution of penton base observed after cell fractionation (Fig. 1a, lanes 9–11).

Five mutants with various phenotypes were also quantitatively analyzed for their cell uptake and localization. Mutant K288E340 carried two substitutions in the integrin binding motifs RGD and LDV (Karayan et al., 1997). Only 10% of K288E340 penton base was found in the vesicular compartment, viz, five times less than WT (Table 1). This was consistent with an integrin binding-defective phenotype, in which integrin-mediated endocytosis would be impaired, as was confirmed by confocal laser immunofluorescence data shown below (refer to Fig. 6b). However, K288E340 was still found in significant amounts in the cytoplasm and nucleus under the EM (Table 1), suggesting the possibility of an alternative

FIG. 5. Immunogold labeling and EM analysis of sections of nuclear membrane and nuclear pores (NP) of HeLa cells incubated with penton base at 37°C for 30 min, as in Fig. 2. Specimens were successively reacted with penton base rabbit antibody and mouse monoclonal antibody (IgM) anti-p62 NP protein, followed by 5-nm gold-conjugated anti-rabbit IgG antibody and 10-nm gold-conjugated anti-mouse IgM antibody. For all panels, except for (b), cytoplasm is on the upper side and nucleoplasm on the lower side of the nuclear membrane section, presented horizontally. In (a) and (b), NP show single labeling with 10-nm gold-labeled anti-p62, with NP viewed in cross (a) or tangential (b) section. Note that in (b), anti-p62 gold grains occupy the central channel position, as shown in a previous study (Wilken *et al.,* 1993). In (c–e), NP are seen with single penton base labeling, in cross (c) and tangential sections (d, e). In (f, g), NP carry double-labeling, with five 10-nm and one 5-nm gold grains in (f) and one 10-nm and six 5-nm gold grains in (g), respectively. Bar represents 50 nm.

entry pathway independent of the RGD and LDV motif-mediated integrin pathway.

Penton base physiologically exists as a pentamer at the vertex of the virion (Nermut, 1984; Stewart *et al.,* 1991). Mutants W119H (tryptophan-to-histidine substitution at position 119), Y553F (tyrosine-to-phenylalanine substitution at position 553), and RRR547EQQ (a triple-substitution mutant in the polybasic signal at position

547) have been found to be defective in penton base pentamerization and accumulated as penton base monomers in insect cells (Karayan *et al.,* 1997). To determine whether the quaternary structure of penton base could influence its entry and compartmentalization in HeLa cells, monomeric penton base proteins of mutants W119H, RRR547EQQ, and Y553F were incubated with HeLa cells at 37°C, and cell samples were analyzed by

TABLE 1

Cellular Distribution of Recombinant Ad2 Penton Base in HeLa Cell Compartments[a]

Penton base (WT or mutant)	Oligomeric status[b]	Intracytoplasmic vesicles (V)	Cytoplasm (C)	Nucleus (N)	Ratio (%) V:C:N
Control HeLa[c]	—	0.0 ($n = 5$; $S = 1.4$)	2.7 ± 1.4 ($n = 5$; $S = 37.2$)	3.2 ± 1.8 $n = 5$; $S = 27.2$)	NA[d]
WT Pb	P	72.8 ± 58.3 ($n = 10$; $S = 2.6$)	32.8 ± 24.7 ($n = 6$; $S = 32.3$)	34.7 ± 31.8 ($n = 5$; $S = 32.0$)	50:25:25
K288E340	P	13.9 ± 14.9 ($n = 7$; $S = 4.5$)	56.9 ± 13.0 ($n = 5$; $S = 78.9$)	66.3 ± 17.0 ($n = 4$; $S = 37.7$)	10:40:50
W119H	M	60.9 ± 45.6 ($n = 4$; $S = 3.9$)	33.5 ± 18.1 ($n = 7$; $S = 83.8$)	34.4 ± 16.8 ($n = 7$; $S = 25.5$)	50:25:25
W165H	P	63.3 ± 54.5 ($n = 8$; $S = 3.6$)	19.1 ± 9.7 ($n = 11$; $S = 56.5$)	18.0 ± 9.5 ($n = 6$; $S = 81.8$)	60:20:20
RRR547EQQ	M	37.6 ± 23.3 ($n = 3$; $S = 2.5$)	62.1 ± 39.3 ($n = 5$; $S = 17.7$)	81.0 ± 30.5 ($n = 5$; $S = 13.6$)	20:35:45
Y553F	M	25.2 ± 13.4 ($n = 11$; $S = 18.8$)	16.7 ± 7.8 ($n = 13$; $S = 90.2$)	18.3 ± 2.2 ($n = 7$; $S = 83.9$)	40:30:30

[a] HeLa cell monolayers were incubated with penton base (WT or mutant) at 37°C for 1 h and analyzed by IEM, as presented in Fig. 2. Quantitative analysis of penton base cellular distribution was performed by counting the colloidal gold grains in the different cell compartments. Results are given as number of gold grains per μm^2 of surface area, $\pm SD$. n, number of separate cell sections analyzed; S, total surface analyzed in μm^2.

[b] The penton base mutant phenotype, with respect to the major protein species recovered (Karayan et al., 1997), is indicated as M (pentamerization-defective monomers) or P (pentamers).

[c] Control HeLa corresponded to cell monolayers incubated with PBS without penton base at 37°C, processed for EM, and reacted with the same primary and gold-labeled secondary antibodies.

[d] NA: background labeling, calculation of the ratio not applicable.

IEM. Cell entry of W119H at 37°C apparently occurred with the same efficiency as WT penton base, with a relative distribution of W119H in the three major cell compartments similar to that of WT penton base (Table 1). The cellular uptake of Y553F monomers seemed to occur with slightly less efficiency than for WT pentamers or W119H monomers, but its pattern of cellular distribution did not significantly differ from those of WT and W119H (Table 1). This implied that the monomeric status of penton base protein had no detrimental effect on its cellular attachment, entry, and nuclear localization in HeLa cells. This also indicated that the peptide motifs involved in these functions were carried by the penton base monomer.

The penton base mutants W119H, W165H, and RRR547EQQ have been found to be phenotypically defective in nuclear addressing in insect cells (Karayan et al., 1997). In HeLa cells, however, W119H showed WT levels of nuclear localization, and RRR547EQQ showed an even higher efficiency than WT (Table 1). This suggested that the N-terminal domain carrying the W119H mutation and the C-terminal polybasic signal at position 547 in penton base were not acting as nuclear localization signals (NLS) in human cells. The higher ratio of nuclear to cytoplasmic gold particles observed with mutant RRR547EQQ might result from its monomeric status, which could facilitate its transport or diffusion, and/or from alteration of some cytoplasmic retention signal(s). W165H carried a tryptophan-to-histidine substitution at position 165 and occurred as a pentamer (Karayan et al.,

1997). Only 20% of W165H penton base molecules were found in the cytosol and the nucleus, versus 60% within vesicles (Table 1). W165H seemed therefore to be phenotypically defective in nuclear transport in HeLa cells, as observed in Sf9 cells.

Cellular requirements for intracellular movement and nuclear import of penton base

The following experiment was designed to determine whether WT penton base could diffuse freely within the cytoplasm to reach the NPC or whether its intracellular movement required cell components or subcellular structures. Immunolocalization of the penton base was thus analyzed in situ using permeabilized cells. HeLa cells were fixed and permeabilized with Triton X-100, incubated with penton base or anti-NPC p62-glycoprotein IgM antibody, and processed for IF or IEM. No penton base labeling could be detected in the vicinity of the nuclear membrane or at the NPC (not shown), whereas NPCs were found to be labeled with anti-p62 colloidal grains (as in Figs. 5a and 5b). Likewise, when WT penton base was incubated with nuclear membranes isolated from HeLa cells under conditions that preserve the NPC architecture (Matunis et al., 1996) and p62 immunoreactivity (Dabauvalle et al., 1988), no penton base binding to the NPC was detected by IF and IEM (data not shown). These results suggested that, contrary to anti-NPC p62 antibodies that bind to the NPC of isolated nuclear envelopes, intracellular vectorial move-
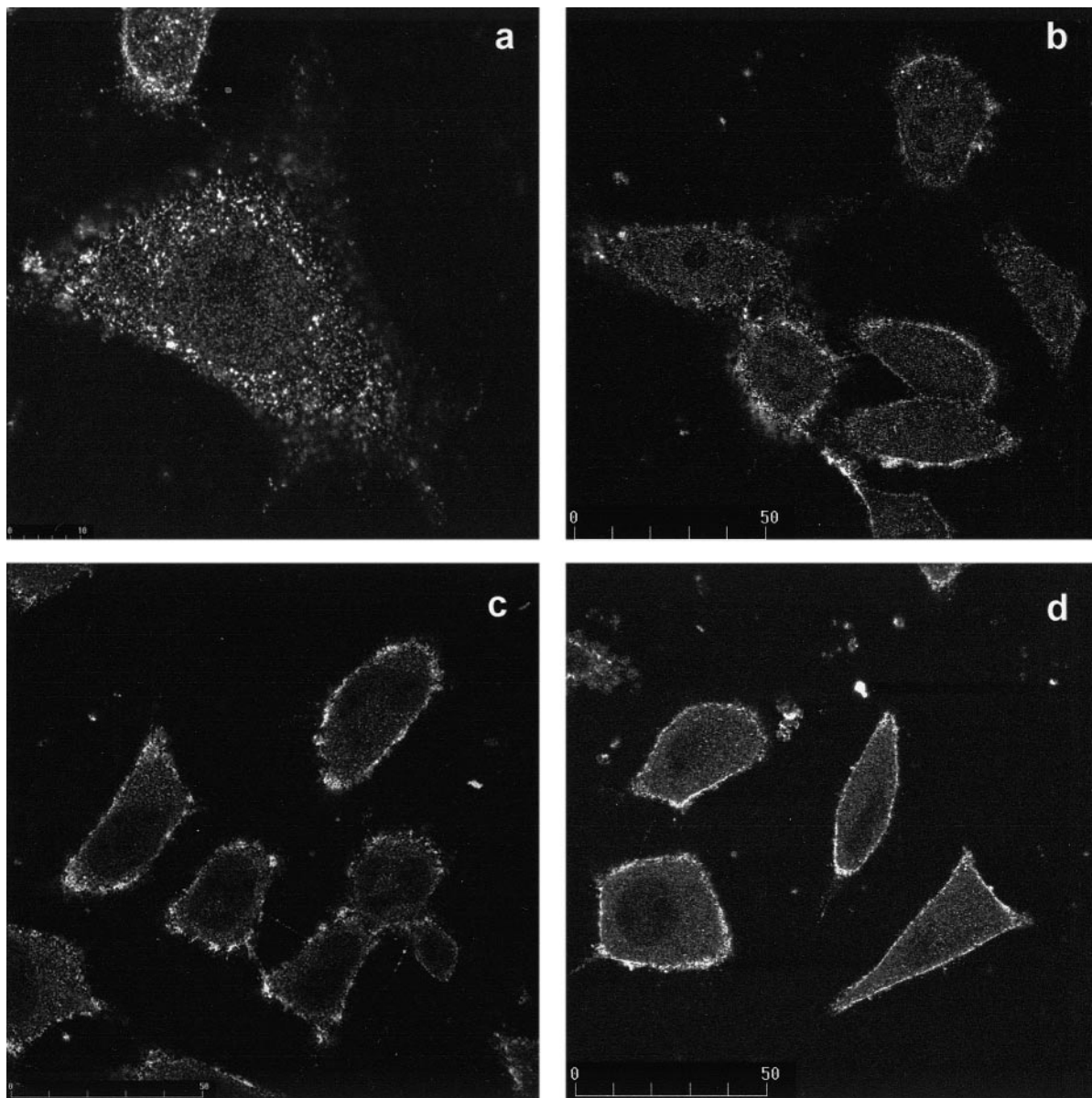
FIG. 6. Effects of cytoskeleton-targeted drugs on cellular compartmentalization of penton base, analyzed by indirect IF in confocal laser microscopy. HeLa cell monolayers, pretreated or not with the drug, were incubated with penton base at 37°C for 30 min, permeabilized, and reacted with anti-penton base antibody and FITC-conjugate. (a) WT penton base with untreated cells; (b) K288E340 mutant with untreated cells; (c) WT penton base with cytochalasin D-treated cells; (d) WT penton base with nocodazole-treated cells.

ment of the penton base to the nucleus, its docking at the NPC, and its nuclear import required the integrity of recipient cells. The next experiments investigated the role of cytoskeletal elements in this process.

The intracellular localization of penton base protein was analyzed under various conditions using penton base antibody and FITC-conjugated anti-IgG in confocal laser IF microscopy. After 30 min of incubation of WT penton base with HeLa cells at 37°C, the cells showed a predominant cytoplasmic fluorescence consisting of large bright speckles visible over a field of diffuse and finely punctuated fluorescence, suggesting both cytoplasmic and vesicular localization. A nuclear fluores-

cence was also detectable, although fainter compared to the cytoplasm (Fig. 6a). The double mutant K288E340 showed a faint cytoplasmic and nuclear fluorescence and a bright halo at the periphery of the cells (Fig. 6b). This pattern suggested a delay in endocytosis and cellular uptake, consistent with the phenotype of this integrin-binding defective mutant protein.

In cells pretreated with the microfilament-disrupting drug cytochalasin D prior to incubation with WT penton base, the fluorescent signal of the penton base formed a bright peripheral ring at the plasma membrane (Fig. 6c). In cells pretreated with nocodazole, a microtubule-depolymerizing drug, and incubated with WT penton base

at 37°C, a similar pattern of peripheral, plasma membrane localization of the penton base fluorescent signal was observed, contrasting with a faint cytoplasmic fluorescence and the absence of nuclear fluorescence (Fig. 6d). IEM analysis confirmed the absence of detectable penton base immunogold labeling in the cytoplasm and nucleus of cytochalasin D- and nocodazole-treated cells (not shown). This suggested that the integrity of actin microfilaments and microtubules was essential for the entry and vectorial movement of penton base toward the nucleus and its nuclear import.

DISCUSSION

It is now generally considered that Ad enters its host cells by endocytosis (Chardonnet and Dales, 1970), a temperature-dependent, receptor-mediated phenomenon, which physiologically occurs at 37°C and requires penton base–integrin interaction (Belin and Boulanger, 1993; White, 1993; Wickham et al., 1993). Functions such as (i) cell binding and endocytosis of Ad particles (Belin and Boulanger, 1993; Mathias et al., 1994; Nemerow et al., 1994; Wickham et al., 1993), (ii) vesicular escape of virions (Seth, 1994a; Wickham et al., 1995), and (iii) endosomal release of coendocytosed toxins (Otero and Carrasco, 1987; Seth et al., 1984) or macromolecules (Defer et al., 1990; Karayan et al., 1997; Seth et al., 1994; Yoshimura, 1985; Yoshimura et al., 1993) have been assigned to the penton base capsomeres present in the Ad capsid. However, no cell trafficking function had been thus far attributed to the isolated penton base protein. In this study, we present biochemical and EM data suggesting that the Ad vertex capsomere devoid of its fiber projection and used as recombinant penton base protein isolated from baculovirus-infected insect cells carries functional domains for (i) its cell attachment, (ii) endocytosis, (iii) vesicular escape, (iv) cytoplasmic transport, (v) passage through the nuclear pore, and (vi) nuclear import, as do infectious adenovirions (Figs. 2, 3, and 6). However, the endosomal release of coendocytosed toxin ricin was three orders of magnitude less efficient for penton base than for adenovirions, for the same amounts of penton base protein involved (Fig. 4). Considering the amount of WT penton base protein occurring within the nucleus, this suggested that endosomolysis was not the only route of cytoplasmic entry for this protein.

Data with pentamerization-defective mutants W119H, RRR547EQQ, and Y553F indicated that pentamerized penton base protein was apparently not required for any of the intracellular steps, suggesting that the peptide domains responsible for these functions were present in the penton base monomer itself. It was reported recently that dodecamers of Ad3 penton base, consisting of the symmetrical arrangement of 12 pentons (also termed dodecahedrons), were capable of cell entry. However, in contrast to our single Ad2 penton base capsomere or its

monomeric subunits, Ad3 dodecamers were blocked at the nuclear pore (Fender et al., 1997), suggesting that the domains responsible for the NPC traverse were probably masked or conformationally altered in the 12-mer edifice. Likewise, Ad2 capsid proteins derived from virions disrupted by heat, pyridine, and mild protease or detergent treatments, as well as complete penton capsomeres (base + fiber) isolated from the cellular pool of soluble proteins, failed to provoke detectable endosome lysis in KB cells, as assayed with EGF-coupled Pseudomonas exotoxin (Seth, 1994b). This suggested that the peptide motifs responsible for the membrane lysis function were highly sensitive to physicochemical modifications of the penton base structure and might not be active in fiber-bound penton base, a situation that has been shown to influence the conformational structure of the penton base (Schoen et al., 1996).

The penton base double mutant K288E340, substituted in both RGD and LDV motifs, showed a peripheral cell localization phenotype in IF (Fig. 6b) and a low level of endosomal localization in IEM (Table 1). This pattern suggested a defect in endocytosis, consistent with its mutations at two major integrin-binding sites. However, significant quantities of K288E340 mutant protein were seen in the cytoplasm and the nucleus under the EM (Table 1). This implied that K288E340 penton base could interact with HeLa cells via a domain(s) independent of the RGD and LDV motifs and enter the cells via an alternative pathway involving receptors other than the previously identified αv, αM, and $\alpha 4$ integrins. Our data with WT penton base, showing that a significant proportion of penton base protein was still vesicular after 60 min (Fig. 1a), suggested that, if this alternative pathway exists, it would be fully functional only when the preferred integrin-mediated pathway is blocked or slowed. No indication of an entry pathway involving caveolae (Anderson et al., 1992; Parton, 1996) was found in IEM using double labeling with penton base and caveolin antibodies (not shown).

Mutants W119H and RRR547EQQ, which have been found to be defective in nuclear addressing in Sf9 cells (Karayan et al., 1997), localized in the nucleus of HeLa cells at WT levels or higher (Table 1). This suggested that mutant phenotypes could vary with extrinsic factors, such as the cellular context. It also indicated that the region overlapping tryptophan-119 and the C-terminal polybasic signal at position 547 in the penton base had no function as a NLS in human cell lines.

In contrast, W165H was found to localize in the nucleus with a low efficiency (Table 1), as in Sf9 cells (Karayan et al., 1997), and preferentially occurred within the endosomal compartment (Table 1). This pattern suggested that W165H could be altered in its vesicular escape or its transport to the nucleus or both. However, vesicular release of coendocytosed RCA–Tf conjugate took place with the same efficiency as with WT penton

base (data not shown), which seemed to exclude the first hypothesis. The penton base domain involved in the W165H mutation showed sequence homology with WD repeats (Karayan *et al.,* 1997), which are frequently found in proteins with cell trafficking properties (Neer *et al.,* 1994). It also shared structural and functional features with a region of the *Drosophila* Antennapedia DNA-binding homeodomain with membrane translocation capacity (Derossi *et al.,* 1994, 1996). (i) The third helix of the Antennapedia homeodomain and its 16-amino-acid-long derived peptide AntpHD41-58 (referred to as penetratin; Derossi *et al.,* 1994) are internalized by cells in culture in a non-receptor-mediated manner (Derossi *et al.,* 1996), a property that has been used to address biologically active substances to the nucleus of cultured cells (Théodore *et al.,* 1995). (ii) Both proteins contain relatively homologous peptide motifs, QIKIWFQN in AntpHD41-58 and ELKYEWVE within residues 160–167 in the penton base. If the W165H mutation had altered a domain involved in cell trafficking of the penton base, this in turn could provoke a negative feedback effect on its release from the endosomal compartment.

The alteration of the intracellular distribution of penton base by cytochalasin D and nocodazole (Figs. 6c and 6d) suggested that actin cables and microtubules were both involved in its vectorial transport to the nucleus. A reorganization of the actin filament network, termed actin cabling, has already been reported in HeLa cells upon adsorption of Ad2 virions or pentons, but not isolated fibers (Belin and Boulanger, 1993), an observation consistent with the finding that actin cables are connected to the intracytoplasmic domain of the plasma membrane integrins (Ruoshlahti, 1988). Likewise, α-tubulin covalently linked to infecting Ad2 particles has been recovered from BHK-21 cells after *in situ* cross-linking experiments (Belin and Boulanger, 1985), and Ad virions have been found to bind to reconstituted microtubules *in vitro* (Weatherbee *et al.,* 1977). Since the cytoskeletal network is functionally and structurally connected to the cytoplasmic fibrils of the NPC (Davis, 1995; Görlich and Mattaj, 1996; Nigg, 1997; Richardson *et al.,* 1988), it is tempting to speculate that the cytoskeleton could serve to guide the penton base molecules toward the nuclear pore channel. The fact that we were unable to find any detectable interaction between the penton base and the HeLa cell nuclear membrane or NPC in permeabilized cells or in *in vitro* binding assays suggested that cell internalization and binding to cytoskeletal elements of human cells were prerequisite steps for efficient penton base nuclear addressing, docking, and translocation through the NPC.

Biological functions associated with Ad penton base were reminiscent of those of VP22, a tegument protein of herpesvirus HSV-1, which has recently been shown to possess cell trafficking properties. Exported from the cells from which it was synthesized by a nonclassical, Golgi-independent pathway, it was capable of reentering surrounding cells and being delivered to the nucleus where it bound to chromatin and was segregated to daughter cells (Elliott and O'Hare, 1997). Likewise, penton base secreted from Sf9 cells by a Golgi-independent mechanism could enter HeLa cells, and its intracellular movement in the recipient cells depended, at least partially, on the integrity of the actin network. However, in contrast to VP22, the penton base was not maintained in recipient cells after 72 h of culture and was likely eliminated by proteolysis. Despite these differences, both Ad penton base and VP22 proteins offer some clue to the development of new types of nonreplicating, virus-derived vectors. Alternatively, they could be advantageously used as viral probes to dissect molecular mechanisms of cellular events, such as membrane translocation, endosomolysis, or nuclear import of macromolecules through the NPC.

MATERIALS AND METHODS

Recombinant penton base proteins. Ad2 WT recombinant penton base protein (PbFL571) and point mutants K288E340, W119H, W165H, RRR547EQQ, and Y553F were expressed in baculovirus-infected insect cells, as described in detail in previous studies (Karayan *et al.,* 1994, 1997). K288E340 carried a double mutation at positions 288 (D to K substitution) and 340 (R to E substitution). W119H and W165H were two single mutants with a tryptophan-to-histidine substitution at positions 119 and 165, respectively, and Y553F had a conservative mutation (Y to F substitution) at position 553 near the C-terminus. RRR547EQQ was a triple-substitution mutant in the C-terminal polybasic motif at position 547–549. Penton base proteins were isolated from Sf9 cell lysates and purified using a modification of our three-step procedure (Boudin *et al.,* 1979; Boulanger and Puvion, 1973): the first step of ammonium sulfate precipitation was replaced by ultracentrifugation in the sucrose gradient in order to isolate 9S pentameric capsomeres for WT, K288E340, and W165H, and 3S monomers for W119H, RRR54EQQ, and Y553F mutants (Karayan *et al.,* 1994, 1997).

Interaction of Ad2 penton base with HeLa cells. Aliquots of recombinant penton base, WT or mutant (6 μg protein, corresponding to 12×10^{12} penton base molecules), in 300 μl of phosphate-buffered saline (PBS) supplemented with 0.5% BSA were incubated with 10^6 HeLa cells at 37 or 0°C for periods of time ranging from 15 min to 2 h, as indicated. The WT penton base-induced cell-detaching effect (Bai *et al.,* 1993; Boudin and Boulanger, 1982; Karayan *et al.,* 1994, 1997) was reduced to less than 20% of the cell monolayers under these experimental conditions. The remaining cells attached to the solid support were harvested at the times indicated and processed for immunofluorescence, electron and immuno-electron microscopy, or biochemical analysis. Since

there was no significant difference in the cellular distribution of the penton base in the two cell populations, as shown by Western blot analysis, the detached cells were eliminated.

Generation of ricin–transferrin complex and endosomolysis assay. Ricin was coupled to transferrin via a streptavidin bridge. Biotin-labeled ricin agglutinin (RCA120, 120,000 mol wt; Sigma) was mixed with biotin-labeled human transferrin (85,000 mol wt; Sigma) in PBS in an equal molar ratio of biotin groups. In a standard procedure, 8.4 nmol of RCA120 carrying 5.3 mol biotin per mole of lectin, and 6.5 nmol of Tf with 6.7 mol biotin per mole of Tf were mixed, then 22 nmol of streptavidin (Sigma), providing a total number of 88 biotin-binding sites, was added to the mixture. Thus, each mole of streptavidin would statistically carry 2 mol of RCA and 2 mol of Tf. The complex was used at a final input of 1 μg of RCA120 per sample of 10^5 HeLa cells, grown as monolayers. Cells were preincubated with RCA–Tf complex with or without Ad or penton base for 1 h at 37°C, in methionine- and cysteine-deprived culture medium. [^{35}S]Methionine and [^{35}S]cysteine (>1000 Ci/mmol; PRO-MIX; Amersham) were added at 15 μCi per 10^5 cells and incubation further proceeded for 1 h at 37°C. Ad2 inoculum was added at a m.o.i. ranging from 0 to 50 PFU/cell, and penton base was added at protein inputs ranging from 0 to 5 μg per 10^5 cells. Cells were then rinsed with culture medium, detached from the support, and dissolved in 0.2N NaOH, 1% SDS. Cellular proteins were precipitated by addition of 10 vol trichloroacetic acid (TCA) at 10% and retained on GF/C glass filters, and TCA-precipitable radioactivity was determined by scintillation counting in a liquid spectrometer (Beckman LS 6500).

Antibodies and reagents for cytology. Penton base rabbit antiserum, raised against WT Ad2 penton base 9S pentamers (laboratory-made; Karayan *et al.,* 1994, 1997), and monoclonal antibody directed against the p62 nuclear pore glycoprotein (mouse IgM; Dabauvalle *et al.,* 1988; Starr *et al.,* 1990) have been described in previous studies. Anti-penton base monoclonal antibodies (mouse IgG) 5A5 and 1D2 were kindly provided by Marc Eloit (Ecole Nationale Vétérinaire, Maisons-Alfort). Anti-caveolin 11.1-kDa cytoplasmic domain rabbit antibody was purchased from Transduction Laboratories (Lexington, KY). Fluorescein isothiocyanate (FITC)-conjugated, affinity-purified, goat anti-rabbit or anti-mouse IgG antibodies were obtained from Jackson ImmunoResearch (West Grove, PA). The cytoskeleton targeted drugs cytochalasin D, used at 1 μM, and nocodazole, used at 10 μg/ml, were both purchased from Sigma. They were added to HeLa cell cultures for 1 h at 37°C prior to penton base addition at 20 μg/ml in PBS.

Electron microscopy and immunoelectron microscopy. Cell specimens were processed for inclusion in epoxy resin (Epon), as previously described (Carrière *et al.,*

1995; Huvent *et al.,* 1998). Hydrophobic resin Epon was preferred to hydrophilic resin metacrylate in the present study for the following reasons: (i) it allowed better morphological analyses than metacrylate resins (Lowicryl) in conventional EM and IEM; (ii) most penton base antigenic epitopes apparently resisted the Epon inclusion and etching processes and still reacted with our polyclonal anti-penton base antibody in IEM (Karayan *et al.,* 1994, 1997). Indirect visualization of cell-associated penton base molecules on cell sections was performed by incubation with primary penton base rabbit antibody diluted at 1:150 in Tris-buffered saline (TBS), followed by a secondary 5-nm colloidal gold-labeled anti-rabbit IgG antibody (Amersham) at 1:50 in TBS for 3 h at room temperature (RT). For double immunogold labeling, sections were postincubated with unlabeled goat anti-rabbit IgG at 1:50 in TBS overnight at 4°C to quench any possible nonspecific reaction with the antibody of the first labeling step. Sections were then incubated with anti-p62 nuclear pore glycoprotein at 1:100 in TBS overnight at 4°C, followed by 10-nm colloidal gold-labeled anti-mouse IgM antibody (British BioCell International, Cardiff, UK) at 1:50 in TBS for 3 h at RT. Specimens were examined under the Hitachi HU-7100 electron microscope. Cell compartments were quantitatively analyzed for immunogold labeling by manual counting of grains under a magnification glass and confirmed by scanning of EM photographs, using an image analyzer (Agfa Arcus2-PCF) and the NIH Image program, version 1.60.

Gold labeling of penton base. Penton base was tagged with colloidal gold for direct visualization of cell-associated penton base molecules under the EM. Gold colloid (10 nm in diameter) was purchased from British BioCell International. Gold labeling of penton base protein was carried out according to the method of De Mey (1983) with the following modification: the reaction medium was adjusted to pH 5.85, i.e., the isoelectric pH of Ad2 penton base (Lemay and Boulanger, 1980), as recommended by the manufacturer.

Immunofluorescence microscopy. HeLa cells treated with penton base were fixed with 2% paraformaldehyde and permeabilized with 0.1% Triton X-100 before being processed for IF microscopy. After being blocked with 1% bovine serum albumin in PBS for 30 min at room temperature, the cells were first incubated with penton base rabbit antibody diluted at 1:1000 in PBS, followed by the secondary, FITC-labeled anti-rabbit antibody (Sigma) diluted at 1:100. Cellular localization of penton base protein was analyzed using a confocal microscope (Bio-Rad 1024). Optical sections of 0.35 μm in thickness were sampled through the cell monolayers and images were scanned at 512 × 512 pixel resolution.

Flow cytometry. Cell viability was analyzed by flow cytometry, performed by differential cell labeling using Hoechst 33342 reagent and propidium iodine, in a FAC-

Scan flow cytometer (Becton Dickinson, Mountain View, CA).

Biochemical and immunological analyses. Cells were refrigerated in ice and lysed in precooled hypotonic buffer, and all subsequent steps of cell fractionation were conducted at 4°C to minimize further transport processes between cell compartments. Cell lysates were fractionated using a conventional differential centrifugation method, yielding three subcellular fractions: nuclei, recovered in the pellet at 1000g for 10 min (referred to as fraction N), endosomal vesicles, lysosomes, large organelles, and mitochondria (referred to as V) at 10,000g for 30 min, and the final supernatant (C), consisting of cytosol with ribosomes and endoplasmic reticulum. Each fraction was analyzed by SDS–PAGE and immunoblotting using penton base polyclonal or monoclonal primary antibody and peroxidase- or phosphatase-conjugated anti-rabbit or anti-mouse IgG secondary antibody (Sigma). Immunological quantification of penton base protein on blots was carried out using luminescent substrate (SuperSignal, Pierce) or ^{125}I-labeled secondary antibody (750–3000 Ci/mmol; 5–20 mCi/mg antibody; Amersham) at 3 to 5 μCi/200-cm^2 blot and autoradiography. Radioactively labeled penton base bands were excised from the blots and the radioactivity was determined by liquid scintillation counting, using a liquid spectrometer (LS-5000, Beckman) as previously described (Huvent *et al.,* 1998).

HeLa cell permeabilization and isolation of nuclei and nuclear envelopes. For immunolocalization *in situ,* HeLa cells fixed with 2% paraformaldehyde and permeabilized with 0.1% Triton X-100 were incubated with penton base (100 μg/ml in PBS) for 1 h at 20°C. For *in vitro* binding assays, nuclei from HeLa cells were isolated as described by Krohne *et al.* (1981). Nuclear envelopes were isolated essentially as described by Matunis *et al.* (1996) and incubated with penton base under the same conditions as described above, using envelopes from 1×10^6 nuclei per sample. Possible penton base–NPC interaction was assessed by IF and IEM microscopy.

ACKNOWLEDGMENTS

REFERENCES

Anderson, R. G. H., Kamen, B. A., Rothberg, K. G., and Lacey, S. W. (1992). Potocytosis: Sequestration and transport of small molecules by caveolae. *Science* **255,** 410–411.

Bai, M., Harfe, B., and Freimuth, P. (1993). Mutations that alter an Arg-Gly-Asp (RGD) sequence in the adenovirus type 2 penton base protein abolish its cell-rounding activity and delay virus reproduction in flat cells. *J. Virol.* **67,** 5198–5205.

Belin, M. T., and Boulanger, P. (1985). Cytoskeletal proteins associated with intracytoplasmic human adenovirus at an early stage of infection. *Exp. Cell Res.* **160,** 356–370.

Belin, M. T., and Boulanger, P. (1987). Processing of vimentin occurs during the early stages of adenovirus infection. *J. Virol.* **61,** 2559–2566.

Belin, M. T., and Boulanger, P. (1993). Involvement of cellular adhesion sequences in the attachment of adenovirus to HeLa cell surface. *J. Gen. Virol.* **74,** 1485–1497.

Bergelson, J. M., Cunningham, J. A., Droguett, G., Kurt-Jones, E. A., Krithivas, A., Hong, J. S., Horwitz, M. S., Crowell, R. L., and Weinberg, R. W. (1997). Isolation of common receptor for coxsackie B viruses and adenoviruses 2 and 5. *Science* **275,** 1320–1323.

Boudin, M. L., and Boulanger, P. (1982). Assembly of adenovirus penton base and fiber. *Virology* **116,** 589–604.

Boudin, M. L., Moncany, M., D'Halluin, J. C., and Boulanger, P. (1979). Isolation and characterization of adenovirus type 2 vertex capsomer (penton base). *Virology* **92,** 125–138.

Boulanger, P., and Puvion, F. (1973). Large-scale preparation of soluble adenovirus hexon, penton and fiber antigens in highly purified form. *Eur. J. Biochem.* **39,** 37–42.

Carriére, C., Gay, B., Chazal, N., Morin, N., and Boulanger, P. (1995). Sequence requirements for encapsidation of deletion mutants and chimeras of human immunodeficiency virus type 1 Gag precursor into retrovirus-like particles. *J. Virol.* **69,** 2366–2377.

Chardonnet, Y., and Dales, S. (1970). Early events in the interaction of adenovirus with HeLa cells. I. Penetration of type 5 and intracellular release of the DNA genome. *Virology* **40,** 462–477.

Chroboczek, J., Ruigrok, R. W. H., and Cusack, S. (1995). Adenovirus fiber. *In* "The Molecular Repertoire of Adenoviruses, I, Virion Structure and Infection" Current Topics in Microbiology and Immunology, Vol. 199, pp. 165–200, Springer-Verlag, Berlin/Heidelberg.

Curiel, D. T., Agarwal, S., Wagner, E., and Cotten, M. (1991). Adenovirus enhancement of transferrin-polylysine-mediated gene delivery. *Proc. Natl. Acad. Sci. USA* **88,** 8850–8854.

Dabauvalle, M.-C., Benavente, R., and Chaly, N. (1988). Monoclonal antibodies to a M_r 68,000 pore complex glycoprotein interfere with nuclear uptake in *Xenopus* oocytes. *Chromosoma* **97,** 183–197.

Dales, S., and Chardonnet, Y. (1973). Early events in the interaction of adenovirus with HeLa cells. IV. Association with microtubules and the nuclear pore complex during vectorial movement of the inoculum. *Virology* **56,** 465–483.

Davies, D. R., and Padlan, E. A. (1990). Antibody–antigen complexes. *Annu. Rev. Biochem.* **59,** 439–473.

Davis, L. I. (1995). The nuclear pore complex. *Annu. Rev. Biochem.* **64,** 865–896.

Defer, C., Belin, M. T., Caillet-Boudin, M. L., and Boulanger, P. (1990). Human adenovirus–host cell interactions: A comparative study with members of subgroups B and C. *J. Virol.* **64,** 3661–3673.

De Mey, J. (1983). The preparation of immunoglobulin gold conjugates (IGS reagents) and their use as markers for light and electronmicroscopic immunocytochemistry. *In* "Immunohistochemistry" (A. C. Cuello, Ed.), pp. 347–372. Wiley, Chichester.

Derossi, D., Calvet, S., Trembleau, A., Brunissen, A., Chassaing, G., and Prochiantz, A. (1996). Cell internalization of the third helix of the

Antennapedia homeodomain is receptor-independent. *J. Biol. Chem.* **271,** 18188–18193.

Derossi, D., Joliot, A., Chassaing, A., and Prochiantz, A. (1994). The third helix of the Antennapedia homeodomain translocates through biological membranes. *J. Biol. Chem.* **269,** 10444–10450.

D'Souza, S. E., Haas, T. A., Piotrowicz, R. S., Byers-Ward, V., McGrath, D. E., Soule, H. R., Cierniewski, C., Plow, E. F., and Smith, J. W. (1994). Ligand and cation binding are dual functions of a discrete segment of the integrin b3 subunit: Cation displacement is involved in ligand binding. *Cell* **79,** 659–667.

Elliott, G., and O'Hare, P. (1997). Intercellular trafficking and protein delivery by a herpesvirus structural protein. *Cell* **88,** 223–233.

Endo, Y., and Tsurugi, K. (1987). RNA *N*-glycosidase activity of ricin A-chain. Mechanism of action of the toxic lectin ricin on eukaryotic ribosomes. *J. Biol. Chem.* **262,** 8128–8130.

Fender, P., Ruigrok, R. W. H., Gout, E., Buffet, S., and Chroboczek, J. (1997). Adenovirus dodecahedron, a new vector for human gene therapy. *Nat. Biotechnol.* **15,** 52–56.

FitzGerald, D. J. P., Padmanabhan, R., Pastan, I., and Willigham, M. C. (1983a). Adenovirus-induced release of epidermal growth factor and *Pseudomonas* toxin into the cytosol of KB cells during receptor-mediated endocytosis. *Cell* **32,** 607–617.

FitzGerald, D. J. P., Trowbridge, I. S., Pastan, I., and Willigham, M. C. (1983b). Enhancement of toxicity of antitransferrin receptor antibody–*Pseudomonas* exotoxin conjugates by adenovirus. *Proc. Natl. Acad. Sci. USA* **80,** 4134–4138.

Görlich, D., and Mattaj, I. W. (1996). Nucleocytoplasmic transport. *Science* **271,** 1513–1518.

Greber, U. F., and Kasamatsu, H. (1996). Nuclear targeting of SV40 and adenovirus. *Trends Cell Biol* **6,** 189–195.

Greber, U. F., Willetts, M., Webster, P., and Helenius, A. (1993). Stepwise dismantling of adenovirus 2 entry into cells. *Cell* **75,** 477–486.

Hong, S. S., and Boulanger, P. (1995). Protein ligands of the human adenovirus type 2 outer capsid identified by biopanning of a phage-displayed peptide library on separate domains of wild-type and mutant penton capsomers. *EMBO J.* **14,** 4714–4727.

Hong, S. S., Karayan, L., Tournier, J., Curiel, D. T., and Boulanger, P. (1997). Adenovirus type 5 fiber knob binds to the MHC class I alpha-2 domain at the surface of human epithelial and B lymphoblastoid cells. *EMBO J.* **16,** 2294–2306.

Huang, S., Kamata, T., Takada, Y., Ruggeri, Z. M., and Nemerow, G. R. (1996). Adenovirus interaction with distinct integrins mediates separate events in cell entry and gene delivery to hematopoietic cells. *J. Virol.* **70,** 4502–4508.

Huvent, I., Hong, S. S., Fournier, C., Gay, B., Tournier, J., Carriére, C., Courcoul, M., Vigne, R., Spire, B., and Boulanger, P. (1998). Interaction and co-encapsidation of human immunodeficiency virus type 1 Gag and Vif recombinant proteins. *J. Gen. Virol.* **79,** 1069–1081.

Hynes, R. O. (1992). Integrins: Versatility, modulation and signaling in cell adhesion. *Cell* **69,** 11–25.

Karayan, L., Gay, B., Gerfaux, J., and Boulanger, P. (1994). Oligomerization of recombinant penton base of adenovirus type 2 and its assembly with fiber in baculovirus-infected cells. *Virology* **202,** 782–796.

Karayan, L., Hong, S. S., Gay, B., Tournier, J., Dupuy d'Angeac, A., and Boulanger, P. (1997). Structural and functional determinants in adenovirus type 2 penton base recombinant protein. *J. Virol.* **71,** 8678–8689.

Krasnykh, V. N., Mikheeva, G. V., Douglas, J. T., and Curiel, D. T. (1996). Generation of recombinant adenovirus vectors with modified fibers for altering viral tropism. *J. Virol.* **70,** 6839–6846.

Krohne, G., Dabauvalle, M.-C., and Franke, W. W. (1981). Cell type specific differences in protein composition of nuclear pore complex-lamina structures in oocytes of *Xenopus laevis*. *J. Mol. Biol.* **151,** 121–141.

Lemay, P., and Boulanger, P. (1980). Physicochemical characteristics of structural and nonstructural proteins of human adenovirus type 2. *Ann. Virol.* **131,** 259–275.

Louis, N., Fender, P., Barge, A., Kitts, P., and Chroboczek, J. (1994). Cell-binding domain of adenovirus serotype 2 fiber. *J. Virol.* **68,** 4104–4106.

Mathias, P., Wickham, T., Moore, M., and Nemerow, G. (1994). Multiple adenovirus serotypes use αV integrins for infection. *J. Virol.* **68,** 6811–6814.

Matunis, M. J., Coutavas, E., and Blobel, G. (1996). A novel ubiquitin-like modification modulates the positioning of the Ran-GTPas-activating protein RanGAP1 between the cytosol and the nuclear pore complex. *J. Cell Biol.* **135,** 1457–1470.

Morgan, C., Rosenkranz, H. S., and Mednis, B. (1969). Structure and development of viruses as observed in the electron microscope. X. Entry and uncoating of adenovirus. *J. Virol.* **4,** 777–796.

Neer, E. J., Schimdt, C. J., Nambudripad, R., and Smith, T. F. (1994). The ancient regulatory-protein family of WD-repeat proteins. *Nature* **371,** 297–300.

Nemerow, G. R., Cheresh, D. A., and Wickham, T. J. (1994). Adenovirus entry into host cells: A role for αv integrins. *Trends Cell Biol.* **4,** 52–55.

Nermut, M. V. (1984). The architecture of adenoviruses. *In* "The Adenoviruses" (H. S. Ginsberg, Ed.), pp. 5–34. Plenum, New York.

Neuman, R., Chroboczek, J., and Jacrot, B. (1988). Determination of the nucleotide sequence for the penton-base gene of human adenovirus type 5. *Gene* **69,** 153–157.

Nigg, E. A. (1997). Nucleocytoplasmic transport: Signals, mechanisms and regulation. *Nature* **386,** 779–787.

Olsnes, S., and Phil, A. (1982). *In* "Molecular Action of Toxins and Viruses" (P. Cohen and van Heyningen, Eds.), pp. 51–105. Elsevier, Amsterdam.

Otero, N. J., and Carrasco, L. (1987). Proteins are co-internalized with virion particles during early infection. *Virology* **160,** 75–80.

Parton, R. G. (1996). Caveolae and caveolins. *Curr. Opin. Cell Biol.* **8,** 542–546.

Richardson, W. D., Mills, A. D., Dilworth, S. M., Laskey, R. A., and Dingwall, C. (1988). Nuclear protein migration involves two steps: Rapid binding at the nuclear envelope, followed by slower translocation through nuclear pores. *Cell* **52,** 655–664.

Roelvink, P. W., Lizonova, A., Lee, J. G. M., Li, Y., Bergelson, J. M., Finberg, R. W., Brough, D. E., Kovesdi, I., and Wickham, T. J. (1998). The coxsackievirus–adenovirus receptor protein can function as a cellular attachment protein for adenovirus serotypes from subgroups A, C, D, E, and F. *J. Virol.* **72,** 7909–7915.

Ruoslahti, E. (1988). Fibronectin and its receptors. *Ann. Rev. Biochem.* **57,** 375–413.

Ruigrok, R. W. H., Barge, A., Albiges-Rizo, C., and Dayan, S. (1990). Structure of adenovirus fibre. II. Morphology of single fibres. *J. Mol. Biol.* **215,** 589–596.

Santis, G., Legrand, V., Hong, S. S., Davison, E., Kirby, I., Imler, J. L., Finberg, R. W., Bergelson, J. M., Mehtali, M., and Boulanger, P. (1999). Molecular determinants of adenovirus serotype 5 fibre binding to its cellular receptor CAR. *J. Gen. Virol.* **80,** 1519–1527.

Saphire, A. C. S., Nemerow, G. R., and Gerace, L. (1995). "Adenovirus Docking at the Nuclear Pore Complex by an NLS-Mediated Pathway," American Society for Cell Biology, Annual Meeting Report, p. 1822.

Schoen, G., Fender, P., Chroboczek, J., and Hewat, E. A. (1996). Adenovirus 3 penton dodecahedron exhibits structural changes of the base on fibre binding. *EMBO J.* **15,** 6841–6846.

Seth, P. (1994a). Adenovirus-dependent release of choline from plasma membrane vesicles at an acidic pH is mediated by the penton base protein. *J. Virol.* **68,** 1204–1206.

Seth, P. (1994b). Mechanism of adenovirus-mediated endosome lysis: Role of intact adenovirus capsid structure. *Biochem. Biophys. Res. Commun.* **205,** 1318–1324.

Seth, P., FitzGerald, D., Ginsberg, H. S., Willingham, M., and Pastan, I. (1984). Evidence that the penton base of adenovirus is involved in potentiation of toxicity of *Pseudomonas* exotoxin conjugated to epidermal growth factor. *Mol. Cell. Biol.* **4,** 1528–1533.

Seth, P., FitzGerald, D., Willingham, M., and Pastan, I. (1986). Pathway of

adenovirus entry into cells. *In* "Virus Attachment and Entry into Cells" (R. L. Crowell and K. Lonberg-Holm, Eds.), pp. 191–195. Am. Soc. Microbiol., Washington, DC.

Seth, P., Pastan, I., and Willingham, M. C. (1985). Adenovirus-dependent increase in cell membrane permeability. *J. Biol. Chem.* **260,** 9598–9602.

Seth, P., Rosenfeld, M., Higginbotham, J., and Crystal, R. G. (1994). Mechanism of enhancement of DNA expression consequent to cointernalization of a replication-deficient adenovirus and unmodified plasmid DNA. *J. Virol.* **68,** 933–940.

Starr, C. M., D'Onofrio, M., Park, M. K., and Hanover, J. A. (1990). Primary sequence and heterologous expression of nuclear pore glycoprotein p62. *J. Cell Biol.* **110,** 1861–1871.

Stevenson, S. C., Rollence, M., White, B., Weaver, L., and McClelland, A. (1995). Human adenovirus serotypes 3 and 5 bind to two different cellular receptors via the fiber head domain. *J. Virol.* **69,** 2850–2857.

Stewart, P. L., Burnett, R. M., Cyrklaff, M., and Fuller, S. D. (1991). Image reconstruction reveals the complex molecular organization of adenovirus. *Cell* **67,** 145–154.

Stewart, P. L., Chiu, C. Y., Huang, S., Muir, T., Zhao, Y., Chait B., Mathias, P., and Nemerow, G. R. (1997). Cryo-EM visualization of an exposed RGD epitope on adenovirus that escapes antibody neutralization. *EMBO J.* **16,** 1189–1198.

Stewart, P. L., Fuller, S. D., and Burnett, R. M. (1993). Difference imaging of adenovirus: Bridging the resolution gap between X-ray crystallography and electron microscopy. *EMBO J.* **12,** 2589–2599.

Stouten, P. F. W., Sader, C., Ruigrok, R. W. H., and Cusack, S. (1992). New triple-helical model for the shaft of the adenovirus fibre. *J. Mol. Biol.* **226,** 1073–1084.

Svensson, U. (1985). Role of vesicles during of adenovirus 2 internalization into HeLa cells. *J. Virol.* **55,** 442–449.

Théodore, L., Derossi, D., Chassaing, G., Llirbat, B., Kurbes, M., Jordan, P., Chneiweiss, H., Godement, P., and Prochiantz, A. (1995). Intraneuronal delivery of protein kinase C pseudosubstrate leads to growth cone collapse. *J. Neurosci.* **15,** 7158–7167.

Tomko, R. P., Xu, R., and Philipson, L. (1997). HCAR and MCAR: The human and mouse cellular receptors for subgroup C adenoviruses and group B coxsackieviruses. *Proc. Natl. Acad. Sci. USA* **94,** 3352–3356.

Varga, M. J., Weibull, C., and Everitt, E. (1991). Infectious entry pathway of adenovirus type 2. *J. Virol.* **65,** 6061–6070.

Wang, K., Huang, S., Kapoor-Munshi, A., and Nemerow, G. (1998). Adenovirus internalization and infection requires dynamin. *J. Virol.* **72,** 3455–3458.

Weatherbee, J. A., Luftig, R. B., and Weihing, R. R. (1977). Binding of adenovirus to microtubules. II. Depletion of high-molecular-weight microtubule-associated protein content reduces specificity of in vitro binding. *J. Virol.* **21,** 732–742.

White, J. M. (1993). Integrins as virus receptors. *Curr. Biol.* **3,** 596–599.

Whittaker, G. R., and Helenius, A. (1998). Nuclear import and export of viruses and virus genomes. *Virology* **246,** 1–23.

Wickham, T. J., Filardo, E. J., Cheresh, D. A., and Nemerow, G. R. (1994). Integrin $\alpha v \beta 5$ selectively promotes adenovirus-mediated cell membrane permeabilization. *J. Cell Biol.* **127,** 257–264.

Wickham, T. J., Mathias, P., Cheresh, D. A., and Nemerow, G. R. (1993). Integrins $\alpha v \beta 3$ and $\alpha v \beta 5$ promote adenovirus internalization but not virus attachment. *Cell* **73,** 309–320.

Wickham, T. J., Carrion, M. E., and Kovesdi, I. (1995). Targeting of adenovirus penton base to new receptors through replacement of its RGD motif with other receptor-specific peptide motifs. *Gene Ther.* **2,** 750–758.

Wickham, T. J., Segal, D. M., Roelvink, P. W., Carrion, M. E., Lizonova, A., Lee, G. M., and Kovesdi, I. (1996). Targeted adenovirus gene transfer to endothelial and smooth muscle cells by using bispecific antibodies. *J. Virol.* **70,** 6831–6838.

Wilken, N., Kossner, U., Sénécal, J.-L., Scheer, U., and Dabauvalle, M. C. (1993). Nup180, a novel nuclear pore complex protein localizing to the cytoplasmic ring and associated fibrils. *J. Cell Biol.* **123,** 1345–1354.

Xia, D., Henry, L., Gerard, R. D., and Deisenhofer, J. (1995). Structure of the receptor binding domain of adenovirus type 5 fiber protein. *In* "The Molecular Repertoire of Adenoviruses, I, Virion Structure and Infection" (W. Doerfler and P. Böhm, Eds.), Current Topics in Microbiology and Immunology, Vol. 199, pp. 39–46, Springer-Verlag, Berlin/Heidelberg.

Yoshimura, A. (1985). Adenovirus-induced leakage of co-endocytosed macromolecules into the cytosol. *Cell Struct. Funct.* **10,** 391–404.

Yoshimura, K., Rosenfeld, M. A., Seth, P., and Crystal, R. (1993). Adenovirus-mediated augmentation of cell transformation with unmodified plasmid vectors. *J. Biol. Chem.* **268,** 2300–2303.

Zhai, Z., Wang, X., and Qian, X. (1988). Nuclear-matrix–intermediate filament system and its alteration in adenovirus infected HeLa cells. *Cell Biol. Int. Rep.* **12,** 99–108.

Zhang, Y., and Schneider, R. J. (1994). Adenovirus inhibition of cell translation facilitates release of virus particles and enhances degradation of the cytokeratin network. *J. Virol.* **68,** 2544–2555.